articles

molecular pharmaceutics

Silver Nanoparticles in Therapeutics: Development of an Antimicrobial Gel Formulation for Topical Use

Jaya Jain,[†] Sumit Arora,[†] Jyutika M. Rajwade,[†] Pratibha Omray,[‡] Sanjeev Khandelwal,[‡] and Kishore M. Paknikar*,[†]

Centre for Nanobioscience, Agharkar Research Institute, G. G. Agarkar Road, Pune 411 004, India, and Nano Cutting Edge Technology Pvt. Ltd. 79/87, D. Lad Path, Kalachowki, Mumbai 400 033, India

Received February 12, 2009; Revised Manuscript Received May 25, 2009; Accepted May 27, 2009

Abstract: Silver is an effective antimicrobial agent with low toxicity, which is important especially in the treatment of burn wounds where transient bacteremia is prevalent and its fast control is essential. Drugs releasing silver in ionic forms are known to get neutralized in biological fluids and upon long-term use may cause cosmetic abnormality, e.g., argyria and delayed wound healing. Given its broad spectrum activity, efficacy and lower costs, the search for newer and superior silver based antimicrobial agents is necessary. Among the various options available, silver nanoparticles have been the focus of increasing interest and are being heralded as an excellent candidate for therapeutic purposes. This report gives an account of our work on development of an antimicrobial gel formulation containing silver nanoparticles (SNP) in the size range of 7−20 nm synthesized by a proprietary biostabilization process. The typical minimum inhibitory concentration (MIC) and minimum bactericidal concentration (MBC) against standard reference cultures as well as multidrug-resistant organisms were 0.78−6.25 μg/mL and 12.5 μg/mL, respectively. Gram-negative bacteria were killed more effectively (3 $\log_{10}$ decrease in 5−9 h) than Gram-positive bacteria (3 $\log_{10}$ decrease in 12 h). SNP also exhibited good antifungal activity (50% inhibition at 75 μg/mL with antifungal index 55.5% against *Aspergillus niger* and MIC of 25 μg/mL against *Candida albicans*). When the interaction of SNP with commonly used antibiotics was investigated, the observed effects were synergistic (ceftazidime), additive (streptomycin, kanamycin, ampiclox, polymyxin B) and antagonistic (chloramphenicol). Interestingly, SNP exhibited good anti-inflammatory properties as indicated by concentration-dependent inhibition of marker enzymes (matrix metalloproteinase 2 and 9). The post agent effect (a parameter measuring the length of time for which bacterial growth remains suppressed following brief exposure to the antimicrobial agent) varied with the type of organism (e.g., 10.5 h for *P. aeruginosa*, 1.3 h for *Staphylococcus* sp. and 1.6 h for *Candida albicans*) indicating that dose regimen of the SNP formulation should ensure sustained release of the drug. To meet this requirement, a gel formulation containing SNP (S-gel) was prepared. The antibacterial spectrum of S-gel was found to be comparable to that of a commercial formulation of silver sulfadiazine, albeit at a 30-fold less silver concentration. As part of toxicity studies, localization of SNP in Hep G2 cell line, cell viability, biochemical effects and apoptotic/necrotic potential were assessed. It was found that SNP get localized in the mitochondria and have an IC_{50} value of 251 μg/mL. Even though they elicit an oxidative stress, cellular antioxidant systems (reduced glutathione content, superoxide dismutase, catalase) get triggered and prevent oxidative damage. Further, SNP induce apoptosis at concentrations up to 250 μg/mL, which could favor scarless wound healing. Acute dermal toxicity studies on SNP gel formulation (S-gel) in Sprague−Dawley rats showed complete safety for topical application. These results clearly indicate that silver nanoparticles could provide a safer alternative to conventional antimicrobial agents in the form of a topical antimicrobial formulation.

Keywords: Silver nanoparticles; antimicrobial; formulation; dermal toxicity

Introduction

For thousands of years, silver and silver ions have been used for their bactericidal properties. Ancient Romans treated their water with silver coins, a tradition still being continued in many societies and even in space programs for purifying water aboard the Apollo spacecraft,[1] MIR space station[2] and the Space shuttle.[3] The use of silver as an antimicrobial agent

* Corresponding author. Mailing address: Agharkar Research Institute, Centre for Nanobioscience, G. G. Agarkar Road, Pune 411 004, India. Fax: +91 20 25651542. E-mail: paknikar@vsnl.com.

[†] Agharkar Research Institute.

[‡] Nano Cutting Edge Technology Pvt. Ltd.

(1) Albright, C. F.; Nachum, R.; Lechtman, M. D. Electrolytic silver ion generator for water sterilization in Apollo spacecraft water systems. Apollo applications program. NASA Contract. Rep. 1967; Report Number: NASA-CR-65738.

10.1021/mp900056g CCC: $40.75
Published on Web 05/27/2009

in clinical settings also has a long history. In 1884, Crede, a German obstetrician, used 1% silver nitrate solution to eliminate blindness caused by *postpartum* infections in newborns. In 1920s the US Food and Drug Administration approved colloidal silver for wound treatment. With the advent of antibiotics, in the 1940s, research on medical application of silver declined dramatically. However in 1964, Moyer et al.[4] first used 0.5% silver nitrate solution in the burn arena, which rekindled the research interest in silver. Four years later in 1968, Fox[5] introduced 1% silver sulfadiazine (SSD) cream, which has become one of the leading topical antimicrobial agents used to treat burn wound infections over the last four decades.

At the beginning of 20th century burn wound infections were the major source of morbidity and mortality (over 50%) in burn patients.[6] Burn injury disrupts both the normal skin barrier and many of the systemic host defense mechanisms, which makes skin susceptible to microbial colonization resulting in development of burn wound sepsis. The burned skin remains vulnerable to invasive microbial infections of all kinds until complete epithelial repair has occurred. Overuse of antibiotics and failure to apply basic infection control policies and procedures have contributed to high mortality and morbidity among burn wound patients due to infections caused by multidrug-resistant nosocomial pathogens (e.g., *Pseudomonas aeruginosa*, methicillin resistant staphylococci, vancomycin-resistant enterococci). Thus topical antimicrobial therapy to control colonization and proliferation of microbial pathogens including multidrug-resistant organisms is the most important method of burn wound care. In this respect, antimicrobial agents containing silver (e.g., silver nitrate and silver sulfadiazine) have revolutionized burn wound care and significantly reduced morbidity and mortality.[7]

Silver therapy, in principle, has many beneficial effects such as (a) multilevel antibacterial effect on cells which considerably reduce the chances of developing resistance, (b) effectiveness against multidrug-resistant organisms and (c) low systemic toxicity. However, silver compounds being used for topical applications, viz., silver nitrate and silver sulfadiazine, may get neutralized by anions (chloride, bicarbonate and protein) in body fluids or cause cosmetic abnormality, viz., argyria (blue gray coloration) upon prolonged use, or could arrest the healing process owing to fibroblast and epithelial cell toxicity. Despite these shortcomings, silver sulfadiazine is the most popular topical antimicrobial silver delivery system in use due to nonavailability of safer alternatives.

The present study describes our work on providing an alternative silver delivery system, viz., a silver nanoparticle based topical antimicrobial formulation for indications such as burns and wounds.

Materials and Methods

Synthesis of Silver Nanoparticles (SNP) and Their Characterization. Silver nanoparticles were synthesized by a proprietary process that involves photoassisted reduction of Ag^+ to metallic nanoparticles and their biostabilization (United States Patent No. 7514600). The synthesized nanoparticles were characterized by UV−vis spectroscopy (Nanodrop ND-1000, USA) and high resolution transmission electron microscopy (Philips, Holland CM 200). Particle size distribution was measured by dynamic light scattering (Zetasizer, Malvern Instruments, U.K.). Studies on stability of SNP were carried out by monitoring the changes in surface plasmon resonance characteristics for 8 weeks.

Studies on Bioactivity of SNP. *Antibacterial Activity: Minimum Inhibitory Concentration (MIC), Minimum Bactericidal Concentration (MBC), Time Kill Study, Post Agent Effect (PAE) and Fractional Inhibitory Concentration Index (FICi).* Standard bacterial strains (*Escherichia coli* ATCC 117, *Pseudomonas aeruginosa* ATCC 9027, *Salmonella abony* NCTC 6017, *Salmonella typhimurium* ATCC 23564, *Klebsiella aerogenes* ATCC 1950, *Proteus vulgaris* NCIB 4157, *Staphylococcus aureus* ATCC 6538, *Bacillus subtilis* ATCC 6633 and *Staphylococcus epidermidis* ATCC 1228) and multidrug-resistant (MDR) clinical isolates (eight strains of *Pseudomonas* sp, five strains of *Staphylococcus* sp, six strains of *Escherichia coli* and three strains of *Klebsiella* sp.) were used in the MIC and MBC study.

MIC and MBC were determined by double dilution technique as described in the NCCLS M7-A5 guidelines. Accordingly, 96-well microtiter plates containing 200 μL Muller Hinton (MH) broth (Hi-Media Mumbai, India) with SNP (in the concentration range of 0.78−50 μg/mL) were inoculated with test strains (final cell density of 1×10^5 CFU/mL) and incubated at 37 °C for 24 h. The lowest concentration of SNP showing growth inhibition (as seen visually) was considered as the minimum inhibitory concentration. The minimum bactericidal concentration was recorded as the lowest concentration of SNP that showed no growth on MH agar plates after spot inoculation and incubation for 24 h. Assay was performed in triplicate with appropriate controls (uninoculated medium and medium without SNP).

For time kill study standard bacterial strains and two representative MDR isolates were used. The cultures were inoculated in 2 mL of MH broth (final cell density of 1×10^5 CFU/mL) supplemented with SNP (at concentrations

(2) Conrand, A. H.; Tramp, C. R.; Long, C. J.; Wells, D. C.; Paulsen, A. Q.; Conrand, G. W. Ag^+ alters cell growth, neurite extension, cardiomyocyte beating, and fertilized egg constriction. *Aviat. Space Environ. Med.* **1999**, *70*, 1096–1105.
(3) Melaiye, A.; Youngs, W. J. Silver and its application as an antimicrobial agent. *Expert Opin. Ther. Pat.* **2005**, *15*, 125–130.
(4) Moyer, C. A.; Brentano, L.; Gravens, D. L.; Margraf, H. W.; Monafo, W. W. Treatment of large human burns with 0.5% silver nitrate solution. *Arch. Surg.* **1965**, *90*, 812–867.
(5) Fox, C. L. Silver sulfadiazine: a new topical therapy for Pseudomonas in burns. *Arch. Surg.* **1968**, *96*, 184–188.
(6) Reiss, E. R.; Artz, C. P. Current status of research in treatment of burns. *Mil. Surg.* **1954**, *114*, 187–190.
(7) Fox, C. L., Jr.; Modak, S. M. Mechanism of action of silver sulfadiazine on burn wound infections. *Antimicrob. Agents Chemother.* **1974**, *5*, 582–588.

corresponding to MIC and MBC for the respective cultures) and incubated for 8 h. Aliquots (0.1 mL) were removed at hourly intervals, serially diluted, and total viable counts (TVC) on MH agar plates were determined after incubation at 37 °C for 24 h. Kill curves were constructed by plotting the log CFU against time.

The post agent effect (PAE) was estimated according to a method described by Craig and Gudmundson.[8] One milliliter saline suspensions of standard bacterial strains and two representative MDR isolates (1×10^7 CFU/mL) were exposed to SNP (at concentrations 10 times MIC of respective strains) and incubated at 37 °C for 1 h. At the end of the exposure period, cultures were centrifuged (3000*g* for 5 min) and diluted 1:1000 in nutrient broth. TVC before SNP exposure and immediately after dilution (zero time), and at hourly intervals until tube turbidity reached a No. 1 McFarland standard, were then determined. Growth controls with inoculum but without SNP were included with each experiment. PAE was defined according to the formula PAE = $T - C$, where T is the time required for viability count of an SNP exposed culture to increase by 1 $\log_{10}$ unit above counts taken immediately after dilution and C is the corresponding time for the growth control.

The fractional inhibitory concentration index (FICi) for combination of SNP and commonly used antibiotics (i.e., streptomycin, chloramphenicol, kanamycin, polymyxin B sulfate, ampiclox and ceftazidime) was determined using *Pseudomonas aeruginosa* ATCC 9027. MIC for each of the antibiotics was first estimated, and subsequently, the fractional inhibitory concentration of a combination of drug and SNP was determined by the checkerboard micro titration method[8] in a 96-well microtiter plate using MH broth. The plates were incubated at 37 °C for 18 h, and results were recorded visually as growth/no growth. The FIC was calculated as follows:

$$\mathrm{FIC}_A^* = \frac{\mathrm{MIC}_A \text{ in combination}}{\mathrm{MIC}_A}$$

$$\mathrm{FIC}_B^* = \frac{\mathrm{MIC}_B \text{ in combination}}{\mathrm{MIC}_B}$$

where A = antibiotic and B = SNP

$$\mathrm{FICi} = \mathrm{FIC}_A + \mathrm{FIC}_B$$

The interaction was defined as synergistic if the FICi was ≤0.5, as additive if the FICi was >0.5 to 1.0, as indifferent if the FICi was >1.0 to 2.0, and as antagonistic if the FICi was >2.0.

Antifungal Activity of SNP: MIC, Minimum Fungicidal Concentration (MFC), Time Kill Study and PAE. To assess the antifungal activity of SNP, a laboratory isolate of *Aspergillus niger* was used. The assay was carried out in 100 mm × 15 mm Petri plates containing 4 mL of potato dextrose agar (PDA) supplemented with three different doses of SNP (50, 100, and 200 μg/mL). *A. niger* was spot inoculated on PDA plates, which were then incubated at 28 °C for 72 h. The diameter of the mycelial colony developing on the SNP containing plates was measured and compared with the diameter of the colony obtained on control plates (without SNP). The inhibition of fungal growth was calculated as follows:

$$\text{antifungal index (\%)} = (1 - D_a/D_b) \times 100$$

where D_a is the diameter of the growth zone in the test plates and D_b is the diameter of growth zone in the control plate.

In another experiment, the minimum inhibitory concentration (MIC) of SNP for *C. albicans* ATCC 2091 was determined in 96-well microtiter plates containing 200 μL of YES (yeast extract 0.5 g% and glucose 1 g%, pH 5.6) broth supplemented with SNP (0.78−50 μg/mL) at an initial inoculum density of 2×10^4 CFU/mL. The microtiter plates were incubated at 37 °C and were scored visually for growth/no growth after 24 h.

For time kill study, *C. albicans* was inoculated (final cell density of 2×10^4 CFU/mL) in 2 mL of YES broth supplemented with appropriate amounts of SNP (at concentration corresponding to MIC and MFC) according to the procedure outlined above. The PAE was determined by the viable plate count method as described earlier for the bacterial strains.

Matrix Metalloproteinases (MMP) Inhibition: In Vitro Studies. The gelatinase inhibition test was conducted using a kit based assay (Colorimetric Assay Kit for Drug Discovery—AK-410-A/AK-408-A BIOMOL QuantiZyme Assay System, USA) in a 96-well microtiter plate as per the manufacturer's instructions. Different concentrations of SNP (6.25−100 μg/mL) were added to an assay mixture containing MMP enzyme (MMP-2 or MMP-9; 9 mU/μL). The plates were incubated at 37 °C for 30 min to allow enzyme inhibitor reaction, and then appropriately diluted (in assay buffer) colorimetric substrate (Ac-PLG-[2-mercapto-4-methyl-pentanoyl]-LGOC_2H_5; 100 μM) was added and plates were read at 412 nm in a microplate reader (μQuant, BioTek Instruments, USA). The activity of the enzyme in the presence of SNP was compared to baseline activity (no inhibitor). The assay was also conducted in the presence of an inhibitor (1.3 μM NNGH, a prototype control inhibitor provided with the kit), which served as positive control.

In Vitro Cytotoxicity and Biochemical Mechanisms Involved in Interactions of SNP with Liver Cells. Hep G2 (human hepatocellular carcinoma) cells were obtained from National Center for Cell Sciences (NCCS), Pune, India. Cells were cultured in Dulbecco's modified Eagle's medium supplemented with L-glutamine (4 mM), penicillin (100 units/mL), streptomycin (100 μg/mL) and 10% (v/v) heat inactivated fetal bovine serum (growth medium). Cells were maintained in 5% CO_2 humidified incubator at 37 °C. During subculture, cells were detached by trypsinization when they reached 80% confluency and split (1:4). Growth medium was changed every 3 days.

(8) Craig, W. A.; Gudmundsson, S. The postantibiotic effect. In *Antibiotics in laboratory medicine*, 4th ed.; Lorian, V. Ed., Williams and Wilkins Co.: Baltimore, MD, 1996.

Cell viability was tested using sodium 3′-[1-(phenylaminocarbonyl)-3,4-tetrazolium]-bis (4-methoxy-6-nitro)benzene sulfonic acid hydrate (XTT) assay, based on the cleavage of yellow tetrazolium salt XTT by metabolically active cells to form an orange formazan dye which was quantified using a microplate reader (Biorad, model No. 680). XTT assay was performed according to the manufacturer's instructions with appropriate controls. Cells were seeded in 96-well microtiter plates (1×10^4 cells/200 μL of growth medium/well) followed by overnight incubation. Supernatants from the wells were aspirated out, and fresh aliquots of growth medium (containing SNP in desired concentrations in the range of 3.12−400 μg/mL) were added. After 24 h, supernatants were aspirated out and the cell monolayers in the wells were washed with 200 μL of PBS (0.1 M, pH 7.4). Subsequently, XTT reagent (70 μL) was added in each well and incubated for 5 h, and absorbance at two wavelengths (415 nm for soluble dye and 630 nm for cells) was recorded using the microplate reader. Concentration of SNP showing 50% reduction in cell viability (i.e., IC_{50} value) was then calculated.

For performing transmission electron microscopy, cells were plated into a 35 mm tissue culture plate at a density of 2×10^5 cells (in 2 mL of growth medium). After overnight growth, supernatants from the culture plates were aspirated out and fresh aliquots of growth medium containing $\sim(1/2)IC_{50}$ SNP were added. For control experiments, medium without nanoparticles was used. Upon incubation for 24 h, the cells (about 80% confluent) were trypsinized and pelleted by centrifugation at 500*g* for 5 min. Cell pellets were washed with phosphate buffer (0.1 M, pH 7.4). Cell pellets were fixed using 4% paraformaldehyde and 2.5% glutaraldehyde in 0.1 M phosphate buffer (pH 7.4) for 2 h followed by postfixation in 1% osmium tetroxide (Agar Scientific, Stansted Essex, England, U.K.), for 1.5 h. Cell pellets were dehydrated through a series of ethanol concentrations (20%, 30%, 40%, 50%, 60%, 70%, 90%) followed by treatment with 2% uranyl acetate in 95% ethanol (Enblock stain) for 1 h and further dehydration with 100% ethanol for 1 h. Cell pellets were finally treated with propylene oxide (twice for 15 min each) followed by 1:1 propylene oxide: Araldite resin for overnight. Cell pellets were infiltrated with fresh Araldite resin (3 changes with a gap of 3 to 4 h). Cell pellets were subsequently embedded in Araldite resin at 60 °C for 48 h and ultrathin sections (70−80 nm) were cut with glass knives in an ultramicrotome (LEICA EM UC6, Netherlands). The sections were mounted on copper grids and stained with 1% aqueous uranyl acetate and 0.2% lead citrate.[9] The stained sections were scanned with an electron microscope (Technai G2 Spirit Biotwin, Netherlands) for ultra structural observations at 80 kV.

For biochemical assays preparation of cell extract was done as follows: 75 cm^2 flasks containing 15 mL of growth medium were seeded with ca. 1×10^7 cells. After overnight growth the cells were challenged with $\sim(1/2)IC_{50}$ SNP (125 μg/mL for Hep G2 cells) and incubated for 24 h. The cells (about 80% confluent) were then trypsinized and pelleted by centrifugation at 500*g* for 5 min. The cell pellet was washed with PBS (0.1 M, pH 7.4), resuspended in 500 μL of chilled homogenizing buffer (250 mM sucrose, 12 mM Tris-HCl, 0.1 mM DTT, pH 7.4) and lysed using Dounce homogenizer. The lysate was centrifuged (8000*g*, 10 min, 4 °C), and the supernatant (cell extract) was used in various biochemical assays. Protein concentration in the cell extract was estimated by the Bradford method.[10]

Catalase activity was measured by the method described by Aebi.[11] In this, absorbance (240 nm) of 1 mL of reaction mixture containing 0.8 mL of H_2O_2 phosphate buffer (H_2O_2 diluted 500-fold with 0.1 M phosphate buffer of pH 7), 100 μL of cell extract, and 100 μL of distilled water was recorded for 4 min against blank (H_2O_2 phosphate buffer). Change in absorbance per min (i.e., ΔA_{240}) was then calculated and used in the estimation of enzyme activity (extinction coefficient value used was 39.4 L M^{-1} cm^{-1}).

Superoxide dismutase (SOD) activity was measured according to the method described by Kono.[12] Briefly, the reaction mixture (2.1 mL) contained 1924 μL of sodium carbonate buffer (50 mM), 30 μL of nitrobluetetrazolium (1.6 mM), 6 μL of Triton X-100 (10%) and 20 μL of hydroxylamine-HCl (100 mM). Subsequently 100 μL of cell extract was added and absorbance (560 nm) was read for 5 min against blank (reaction mixture without cell extract). Change in absorbance per min (i.e., ΔA_{560}) was calculated and used in the estimation of enzyme activity (extinction coefficient value used was 9920 L M^{-1} cm^{-1}).

Glutathione peroxidase activity was measured as described by Flohe and Gunzler.[13] The reaction mixture contained 1.2 mL of potassium phosphate buffer (0.1 M, pH 7), 200 μL of GSH (10 mM), 10 μL of sodium azide (200 mM), 200 μL of cell extract and 200 μL of glutathione reductase (2.4 U/mL). Following incubation at 37 °C for 10 min, 200 μL of NADPH (1.5 mM) and 200 μL of H_2O_2 (1.5 mM) were added. Absorbance (340 nm) was recorded for 4 min against blank (reaction mixture sans cell extract), and change in absorbance per min (i.e., ΔA_{340}) was calculated. The enzyme activity was calculated (extinction coefficient value used was 6220 L M^{-1} cm^{-1}).

Total reduced glutathione (GSH) content was measured as described by Saldak and Lindsay.[14] The reaction mixture containing 1.2 mL of EDTA (0.02 M), 1 mL of distilled water, 250 μL of 50% trichloroacetic acid, and 50 μL of

(9) Reynolds, E. S. The use of lead citrate at high pH as an electron-opaque stain in electron microscopy. *J. Cell Biol.* **1963**, *17*, 208–212.

(10) Bradford, M. A. rapid and sensitive method for the quantification of microgram quantities of protein utilizing the principle of protein-dye binding. *Anal. Biochem.* **1976**, *72*, 248–254.

(11) Aebi, H. Catalase. *Methods Enzymol.* **1984**, *2*, 673–684.

(12) Kono, Y. Generation of Superoxide radical during auto-oxidation of dyhydroxylamine and an assay for Superoxide dismutase. *Arch. Biochem. Biophy.* **1978**, *186*, 189–195.

(13) Flohe, L.; Gunzler, W. A. Assays of glutathione peroxidase. *Methods Enzymol.* **1984**, *105*, 114–121.

Tris buffer (0.4 M, pH 8.9) was centrifuged at 300*g* for 15 min. Clear supernatant (500 μL) was mixed with 1 mL of 0.4 M Tris buffer (containing 0.02 M EDTA, pH 8.9), 100 μL of 0.01 M DTNB [5,5′-dithiobis(2-nitrobenzoic acid)] and 100 μL of cell extract. The mixture was incubated at 37 °C for 25 min, and the yellow color developing was read at 412 nm against blank. The enzyme activity was calculated taking the extinction coefficient, 14150 L M^{-1} cm^{-1}.

Lipid peroxidation was estimated as per the method described by Beughe and Aust:[15] a mixture of 100 μL of tris buffer (150 mM, pH = 7.1), 10 μL of ferrous sulfate (100 mM), 10 μL of ascorbic acid (150 mM), 780 μL of distilled water and 100 μL of cell extract was incubated at 37 °C for 15 min. Thiobarbituric acid (0.375%, 2 mL) was then added to the mixture and allowed to react at 100 °C (in water bath) for 15 min. The reaction mixture was then centrifuged (800*g* for 10 min), and supernatant was read at 532 nm against blank. The enzyme activity was calculated (extinction coefficient value used was 156,000 L M^{-1} cm^{-1}).

For the assessment of apoptosis, caspase-3 colorimetric assays were performed using a standard kit (Sigma, USA) to determine the concentrations of SNP inducing apoptosis and necrosis in cells. Further, to visualize apoptotic/necrotic nuclei, cells were seeded on glass coverslips (18 × 18 mm) placed into 35 mm tissue culture plates at a density of 2 × 10^5 cells (in 2 mL of growth medium). After overnight growth, supernatants from the culture plates were aspirated out and fresh aliquots of growth medium containing SNP at desired concentrations ($\sim$(1/2)IC_{50} and $\sim$2 × IC_{50}) were added. Upon incubation for 24 h, cells were washed with PBS and fixed in 4% chilled paraformaldehyde for 20 min and then washed twice with PBS. Cells were stained by adding 1 mL of AO/EB mix (100 μg/mL AO and 100 μg/mL EB in PBS). After 2 min incubation, cells were washed twice with PBS (5 min each) and visualized under a fluorescence microscope (Zeiss Axio star plus, USA) at 400× magnification with excitation filter 480/30 nm. Three independent cell counts (counting a minimum of 100 total cells each) were obtained on the basis of differential staining of the nuclei (live cells have a normal green nucleus; early apoptotic cells have bright green nucleus with condensed or fragmented chromatin; late apoptotic cells display condensed and fragmented orange chromatin; necrotic cells display a structurally normal orange nucleus). These results were supported by confocal laser scanning microscopy (CLSM). For this cells were mounted with antifade mounting medium (Chemicon, USA) and observed (at 400× magnification) under confocal laser scanning microscope (CLSM 510, version 2.01; Zeiss, USA) after excitation at 488 nm. Green fluorescence was detected with a band-pass filter ranging between 505 and 530 nm. Simultaneously, red fluorescence was detected using the long pass filter at 585 nm, and superimposition of both green and red fluorescence generated the final images.

All the above-mentioned assays were carried out three times, independently. The data obtained were expressed in terms of "mean ± standard deviation" values. Wherever appropriate, the data were also subjected to unpaired two tailed Student's *t* test. A value of $p < 0.05$ was considered as significant.

Preparation and Formulation of SNP Containing Gel (S-Gel). In order to use SNP in the form of a topical hydrophilic formulation, two Carbopol based gel formulations, viz., containing final silver concentrations of 0.02 mg/g and 0.1 mg/g, respectively, were prepared. These gel formulations, designated as S-gel, were packaged under sterile conditions, labeled with appropriate details and stored at room temperature for further use.

In Vitro Antibacterial Activity of S-Gel. A standardized antimicrobial sensitivity test was used to evaluate the antibacterial activity of S-gel against standard bacterial cultures and two representative MDR strains. The test was carried out in Muller−Hinton agar plates according to NCCLS guidelines. For comparison, gel without SNP and 1% silver sulfadiazine (Solvay Pharma, India) was used.

Assessment of Toxicity of S-Gel: In Vivo Study. Acute dermal toxicity study was performed following the Organization for Economic Cooperation and Development (OECD) Guidelines for Testing of Chemicals, Section 4, No. 402 L. Sprague−Dawley rats (5 male and 5 female rats, 12 to 14 weeks old, weighing between 203 and 244 g with healthy intact skin and acclimatized to laboratory conditions for 7 days) were used. Approximately 24 h before application, the hair of each rat was closely clipped with an electric clipper to expose the back from the scapular to the lumbar region. S-gel (0.1 mg/g) was applied uniformly at the dose level of 2000 mg/kg and held in contact with the skin with a porous gauze patch. After the exposure period of 24 h, observations on mortality, intoxication, body weight, and necropsy were recorded for a 14 day period.

Results

The silver nanoparticles synthesized by the patented process showed a characteristic surface plasmon peak, at 436 nm (Figure 1). Further, the nanoparticles were spherical and in the size range of 7−20 nm (Figure 2) as revealed by high resolution transmission electron microscopy (HRTEM). The data on particle size distribution revealed the presence of particles in the size range of 6.5 to 43.8 nm, with an average size 16.6 nm. The nanoparticles were found to be stable for over two months.

Results of susceptibility tests with SNP against reference strains are summarized in Table 1. It could be seen that SNP displayed potent antimicrobial activity against both Gram-positive and Gram-negative organisms. The MICs were in the range 1.56−6.25 μg/mL for all the cultures while the MBCs were 12.5 μg/mL with the exception of *S. aureus* ATCC 6538P. In the latter case, MBC could not be

(14) Saldak, J.; Lindsay, R. H. Estimation of total, protein bound and non-protein sulfhydryl groups in tissue with Ellman's reagent. *Anal. Biochem.* **1968**, *25*, 192–205.

(15) Beuge, J. A.; Aust, A. D. Microsomal lipid peroxidation. *Methods Enzymol.* **1978**, *52*, 302–310.

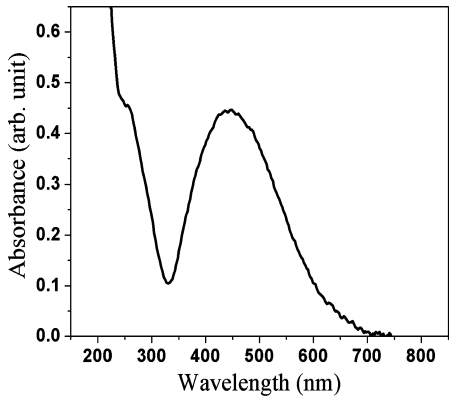

Figure 1. UV−vis absorption spectra of SNP suspension.

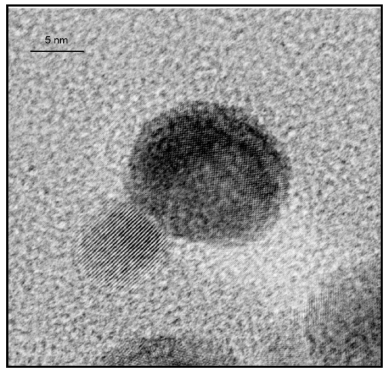

Figure 2. HRTEM of individual SNP.

Table 1. Minimum Inhibitory Concentration (MIC) and Minimum Bactericidal Concentration (MBC) of SNP against Different Organisms

	SNP (μg/mL)		
organisms used	MIC_{50}[a]	MIC_{90}[b]	$MBC_{99.9}$[c]
Pseudomonas aeruginosa ATCC 9027	3.12	6.25	12.5
Salmonella abony NCTC 6017	3.12	6.25	12.5
Salmonella typhimurium ATCC 23564	3.12	6.25	12.5
Klebsiella aerogenes ATCC 1950	1.56	6.25	12.5
Proteus vulgaris NCIB 4157	3.12	6.25	12.5
Bacillus subtilis ATCC 6633	3.12	6.25	12.5
Staphylococcus aureus ATCC 6538	6.25	12.5	ND
Staphylococcus epidermidis ATCC 12228	3.12	6.25	12.5
Escherichia coli ATCC 117	1.56	6.25	12.5

[a] MIC_{50}: minimum inhibitory concentration required to kill 50% of population (scored visually after 14−16 h of incubation). [b] MIC_{90}: minimum inhibitory concentration required to kill 90% of population (scored visually after 24 h of incubation). [c] MBC: minimum bactericidal concentration required to kill 99.9% of population (scored by spot inoculation on MH agar from the wells showing no growth after 24 h). ND: not detectable.

determined because SNP was found to be bacteriostatic even at the highest concentration available for testing, i.e., 50 μg/mL. An analysis of MIC values for standard cultures and MDR strains indicated that the majority of strains, i.e., 66% showed MICs $\leq$ 3.12 μg/mL. Out of these, 4% strains display MIC as low as 0.78 μg/mL. These results show that SNP have a potent antimicrobial activity at very low concentrations.

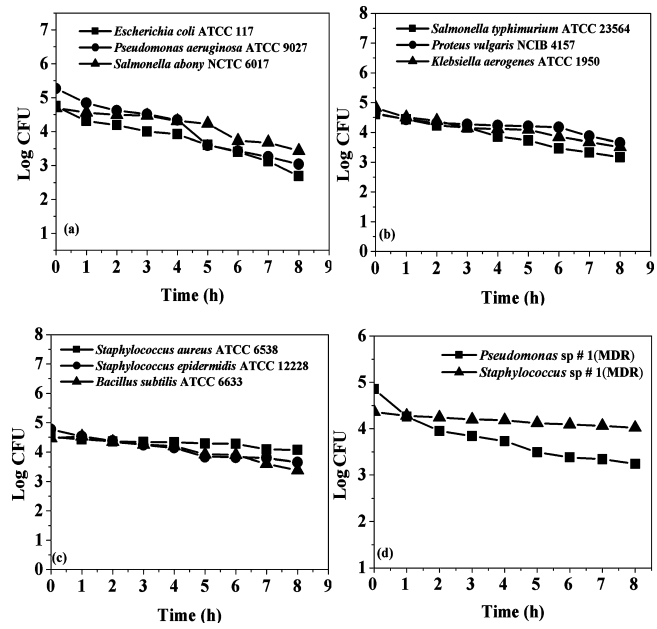

Figure 3. Kill curve of reference bacteria and MDR cultures at MIC of SNP (error bars not shown as deviations from the mean values are <0.1 $\times$ log 10).

Table 2. Microbicidal Activity of SNP at MIC and MBC against Different Bacterial Strains

organism	*D* at MIC[a] (h)	*D** at MBC[b] (h)
Pseudomonas aeruginosa ATCC 9027	3.5	4.7
Escherichia coli ATCC 117	4.4	6
Klebsiella aerogenes ATCC 1950	6.7	9
Salmonella abony NCTC 6017	6.4	9
Salmonella typhimurium ATCC 23564	5.4	7
Proteus vulgaris NCI B 4157	10	8
Bacillus subtilis ATCC 6633	7.17	12
Staphylococcus epidermidis ATCC 12228	7.3	12
Staphylococcus aureus ATCC 6538	18.9	>24
Pseudomans sp. # MDR 1	5.6	4.5
Staphylococcus sp. # MDR 1	>24	>24

[a] D = time required to achieve 1 $\log_{10}$ reduction total viable cell count. [b] D^* = time required to achieve 3 $\log_{10}$ reduction total viable cell count.

As further extension of the MIC and MBC, time kill studies were initiated. Figure 3 demonstrates time-dependent microbicidal action of SNP at MIC. It is evident that Gram-negative bacteria are killed faster than Gram-positive bacteria and there is a linear relationship between log CFU versus time. Slope of the line of regression (K) could be used for the analysis of bactericidal activity of SNP against different microbial species. Data in Table 2 show that the time required to achieve a 1 $\log_{10}$ reduction (D) in viable cells differs with the organisms indicating their varying sensitivity to SNP. At MIC (6.25 μg/mL) time required to achieve 1 $\log_{10}$ reduction (90%) in all tested strains (except *S. aureus*) ranged between 3.5 and 10 h. In general, Gram-negative bacteria were at the lower end and Gram-positive bacteria were at

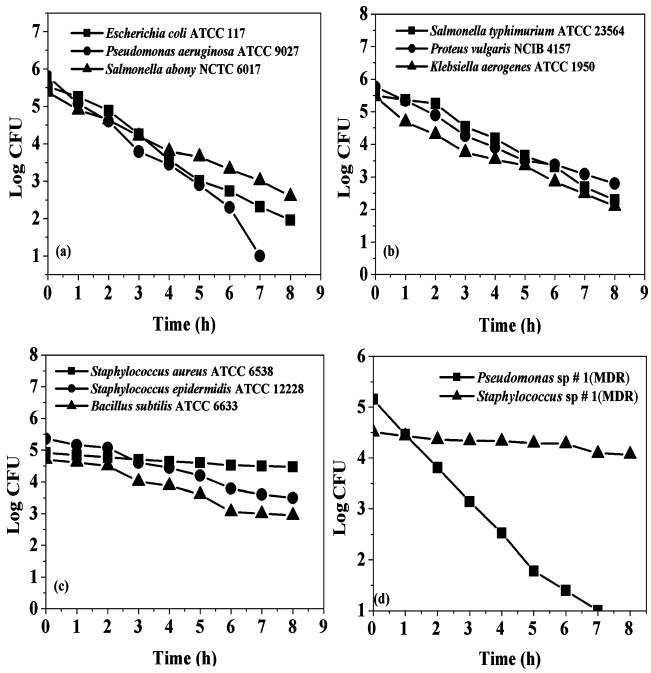

Figure 4. Kill curve of reference bacteria and MDR cultures at MBC of SNP (error bars not shown as deviations from the mean values are <0.1 × log 10).

the higher end of this range. Also, at higher absolute values of *K*, the bactericidal activity was found to be greater. Among all the strains tested, *E. coli* and *P. aeruginosa* were found to be most vulnerable to SNP as they were killed in the least time (3−4 h).

In the next experiment, the time required to achieve 3 $\log_{10}$ decrease in viability level of killing was determined from time kill curves at MBC (12.5 μg/mL) of SNP. The results obtained (Figure 4) clearly show that bactericidal action was more rapid as compared to time kill curves seen at MIC. From the analysis of kill curve the time required to achieve 3 $\log_{10}$ decrease in viable cell count (*D*) was calculated (Table 2). Once again, it is seen that SNP kill Gram-negative bacteria more effectively, achieving a 3 $\log_{10}$ decrease in 5 to 9 h as against 12 h for Gram-positive bacteria such as *B. subtilis* and *S. epidermidis*. Three *Staphylococcus aureus* strains exposed to SNP showed <1 $\log_{10}$ decrease in viability in 8 h and no increase in cell count upon continued incubation for 24 h, suggesting a bacteriostatic effect.

Results obtained for the post agent effect studies are presented in Table 3. The PAE was longer for Gram-negative bacteria than Gram-positive bacteria, with maximum effect against *P. aeruginosa* (PAE 10.5 h) and minimum effect against *Staphylococcus aureus* (PAE 1.3 h). PAE against *E. coli* and *K. aerogenes* could not be measured owing to rapid bactericidal activity while it ranged from 1.3 to 10.5 h for other bacterial strains.

As a part of FIC studies, susceptibility of *P. aeruginosa* to different combinations of SNP and antibiotics was investigated and the results obtained are presented in Table 4. These results clearly show that FICi was synergistic (<0.5) for one combination, i.e., SNP with ceftazidime. Additive

Table 3. PAE on Different Bacterial Strains at Inhibitory (10 × MIC) Concentrations of SNP

organism	PAE (h)
Escherichia coli ATCC 117	NM[a]
Pseudomonas aeruginosa ATCC 9027	10.5
Salmonella abony NCTC 6017	4.6
Salmonella typhimurium ATCC 23564	4.9
Klebsiella aerogenes ATCC 1950	NM
Proteus vulgaris NCIB 4157	8.5
Bacillus subtilis ATCC 6633	3.6
Staphylococcus aureus ATCC 6538	1.3
Streptococcus epidermidis ATCC 12228	1.5
Pseudomonas sp. # MDR 1	9.3
Staphylococcus sp. # MDR 1	1.8

[a] NM = not measurable.

effects (FICi >1) were seen for the individual combination of SNP with streptomycin, kanamycin, ampiclox and polymyxin B. The combination of SNP with chloramphenicol was antagonistic (FICi >2).

SNP were found to inhibit the mycelial growth of *Aspergillus niger* after 72 h of incubation with an IC_{50} value of 75 μg/mL and a corresponding antifungal index of 55.5%. The MIC_{50} and MIC_{90} against *C. albicans* were 6.25 and 12.5 μg/mL, respectively, whereas the MFC of SNP was 25 μg/mL. The data on the time kill studies are presented in Figure 5. At SNP concentrations equal to MIC, 97% of *C. albicans* cells were killed after 8 h of incubation. When *C. albicans* was exposed to higher SNP concentration (MFC), the rate of killing as well as extent of killing increased (99.9%) in 6 h. The PAE of SNP for *C. albicans* was found to be 1.6 h.

Studies on inhibition of matrix metalloproteinase activities show that SNP inhibited MMP-2 and MMP-9 enzymes in a concentration-dependent manner (Figure 6). SNP at concentration of 50 μg/mL showed ~75% inhibition of these enzymes while at 100 μg/mL complete inhibition could be seen.

The interactions of silver nanoparticles were studied in vitro using an established cell line, viz., Hep G2. Data on cell viability estimated by XTT assay (Figure 7) showed a dose-dependent decrease in viability with IC_{50} value working out to be 251 μg/mL. To localize the presence of silver nanoparticles, ultrathin sections of Hep G2 cells exposed to ~(1/2)IC_{50} SNP for 24 h were visualized under transmission electron microscope. Dark, electron dense, spherical aggregates were found inside the mitochondria as compared to unexposed (control) cells (Figure 8, right and left, respectively).

When biochemical changes occurring in the SNP treated cells were monitored (with respect to enzyme activity indicative of oxidative stress), interesting data emerged (Figure 9). Treatment with SNP increased GSH levels by ~1.1-fold (62.09 μmol/mg protein in unexposed cells and 69.12 μmol/mg protein in SNP-exposed cells). There was ~1.1-fold increase in catalase levels after SNP treatment (124.85 μmol/mg protein as compared to 110.17 μmol/mg

Table 4. Susceptibility of *P. aeruginosa* to Individual Agents and Results of Checkerboard Microdilution Studies

drug	MIC (μg/mL)	drug combination MIC (μg/mL)	FICi	interaction
ceftazidime (CF)	0.78	CF (0.39) + SNP (0.78)	0.75	synergistic
streptomycin (ST)	3.12	ST (3.12) + SNP (0.39)	1.125	additive
kanamycin (K)	12.5	K (12.5) + SNP (0.39)	1.125	additive
ampiclox (AC)	1.95	AC (1.95) + SNP (0.39)	1.125	additive
polymyxin B (P)	1.56	P (1.56) + SNP (0.195)	1.0625	additive
chloramphenicol (CHL)	12.5	CHL (25) + SNP (1.56)	2.5	antagonistic
SNP	3.12			

protein in control cells). SOD levels were found to be ~1.4-fold higher for SNP treated cells (4.97 μmol/mg) as compared to unexposed cells (3.47 μmol/mg protein). However, changes observed in the levels of lipid peroxidation and GPx were not statistically significant ($p > 0.05$).

The apoptotic thresholds of SNP were monitored by caspase-3 assay after exposure to SNP for a range of doses (0.39−350 μg/mL), and the results of a representative dose-range study are shown in Figure 10. SNP could induce apoptosis at concentrations in the range of 6.25−250 μg/mL. The study was complemented by microscopic observations on cells. Exposure to 125 μg/mL (~(1/2)IC_{50}) SNP resulted in apoptosis (as evidenced by bright green nucleus with condensed or fragmented chromatin under CLSM, upon AO/EB double staining) of cells (Figure 11B). Further, at SNP concentration 500 μg/mL (~2 × IC_{50}) cells with structurally normal but orange stained nuclei were observed

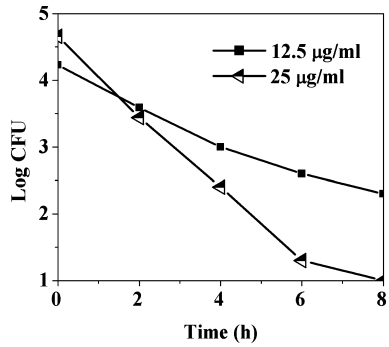

Figure 5. Time kill study performed using SNP against *C. albicans* at MIC and MFC (error bars not shown as deviations from the mean values are <0.1 × log 10).

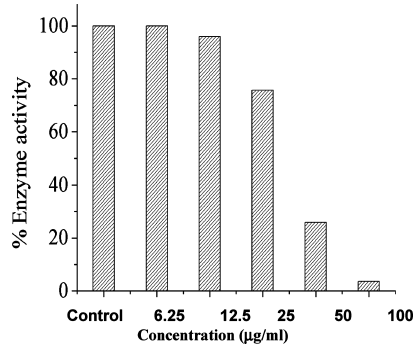

Figure 6. Inhibition of MMP-2 (gelatinase A) enzyme in the presence of SNP (error bars not shown as deviations from the mean values are <1%).

(Figure 11C), suggesting necrosis. Table 5 shows quantitative data on the percentage of live, apoptotic and necrotic cells after exposure to ~(1/2)IC_{50} and ~2 × IC_{50} SNP as compared to control cells which was obtained using fluorescence microscopy after AO/EB double staining. Data showed 67% live cells, 28% apoptotic cells and 5% necrotic cells at SNP concentration of 125 μg/mL (~(1/2)IC_{50}) whereas 53% live cells, 11% apoptotic cells and 36% necrotic cells were noticed at 500 μg/mL SNP concentration (~2 × IC_{50}).

The above experiments demonstrating the antibacterial, antifungal nature of SNP as well as those proving its anti-inflammatory activity, cytotoxicity, intracellular localization and biochemical changes relating to metal stress response were carried out using aqueous a colloidal suspension of SNP. The following paragraphs describe results of the study on gel formulation containing SNP, i.e., S-gel (Figure 12).

Table 6 and Figure 12 show the results of in vitro antibacterial activity of S- gel. The zone of inhibition for S-gel was in the range of 3 to 10 mm at 0.020 mg/g of gel. Maximum antibacterial activity (10 mm) of S-gel was noted against *Pseudomonas* sp. At higher concentration of silver (0.1 mg/g) S-gel showed a significantly wider zone of

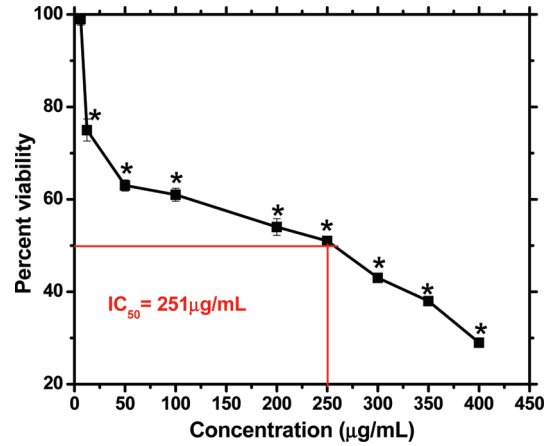

Figure 7. Percent viability measured by XTT assay on Hep G2 cells after treatment with SNP (12.5 μg/mL to 400 μg/mL) for 24 h. The data are expressed as mean ± standard deviation (SD) of three independent experiments. An OD value of control cells (unexposed cells) was taken as 100% viability (0% cytotoxicity). Asterisk (*) denotes a statistically significant difference compared to control ($p < 0.05$).

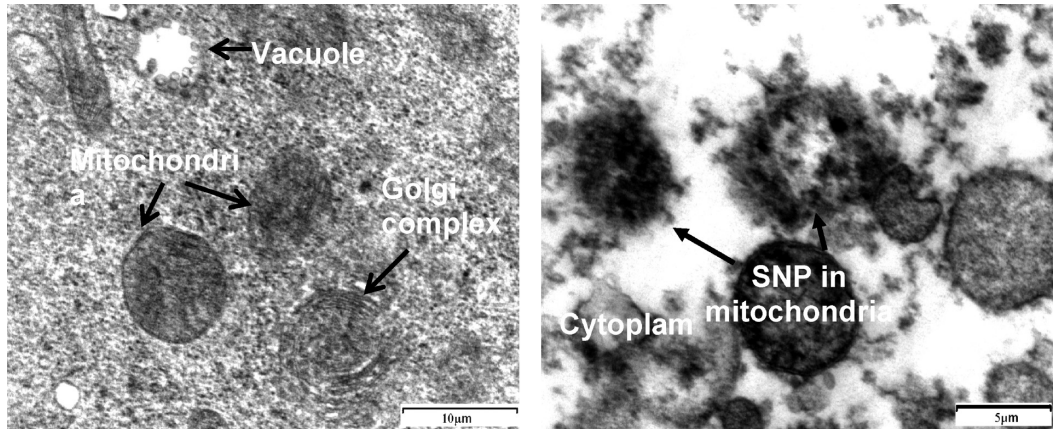

Figure 8. (Left) Transmission electron micrographs of unexposed (control) Hep G2, arrows showing the cellular structures, viz., mitochondria, Golgi complex, vacuole and cytoplasm (scale marker indicates $\times 10$ μm). (Right) Transmission electron micrographs of Hep G2 cells after the cultures were exposed to $\sim(1/2)IC_{50}$ SNP (125 μg/mL) for 24 h, arrows showing the presence of SNP in mitochondria (scale marker indicates $\times 5$ μm).

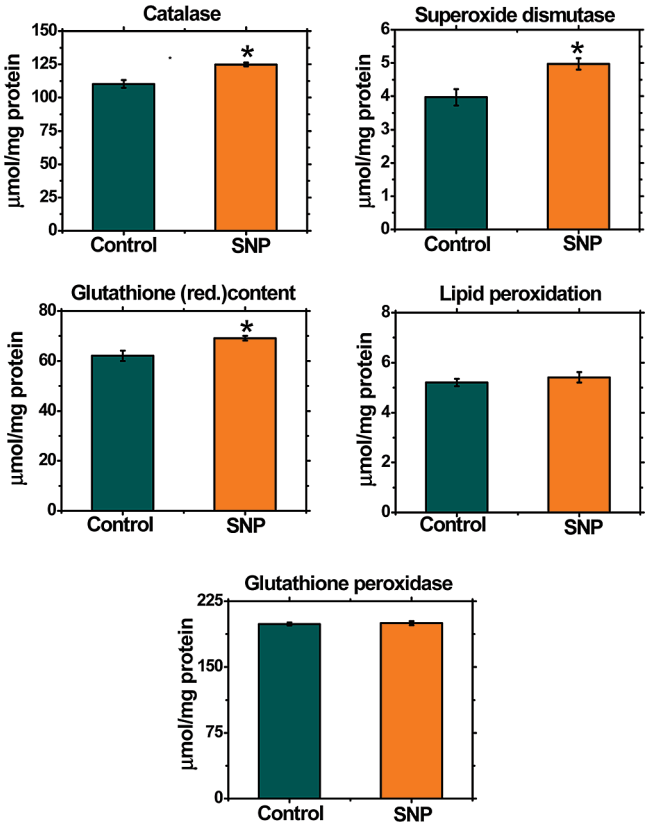

Figure 9. Levels of catalase, super oxide dismutase, reduced glutathione content, lipid peroxidation and glutathione peroxidase in untreated (control: not treated with SNP) and treated (with $\sim(1/2)IC_{50}$ SNP, 125 μg/mL for 24 h) Hep G2 cells. The data are expressed as mean $\pm$ standard deviation (SD) of three independent experiments. Asterisk (*) denotes a statistically significant difference compared to control ($p < 0.05$).

inhibition. Zones of inhibition for SNP and silver sulfadiazine (SSD) against *P. aeruginosa* were of the same size (13 mm). No zone of inhibition was obtained with control gel without silver nanoparticles.

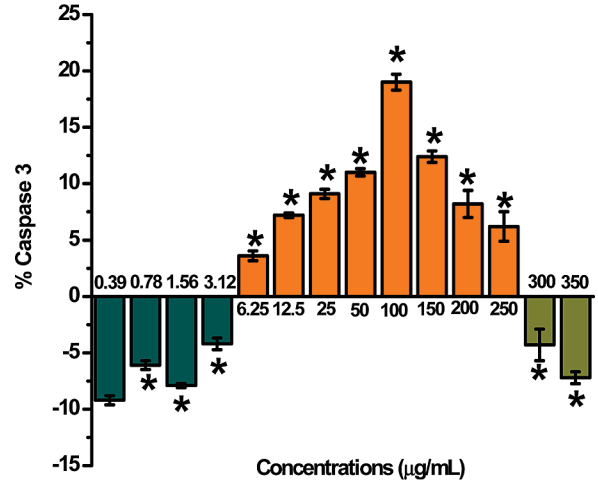

Figure 10. Caspase-3 activity assay for Hep G2 cells. SNP induce caspase-3 production (apoptosis) at concentrations in the range of 6.25−250 μg/mL. An OD value of positive control was taken as 100%. Asterisk (*) denotes a statistically significant difference compared to control ($p < 0.05$).

Since the antibacterial action of SNP in the S-gel formulation was unequivocally demonstrated, further in vivo experiments on the determination of LD_{50} for S-gel were performed in Sprague−Dawley rats. The acute dermal LD_{50} value of S-gel in Sprague−Dawley rats, both male and female, was found to be greater than 2000 mg/kg body weight. No mortality or signs of intoxication or any adverse skin reactions were observed in the treated male and female rats during the observation period of 14 days following application. Gain in body weight of treated animals was normal in the first and second weeks after treatment. At termination of the study, animals were sacrificed and necropsy was performed on all animals. Also, no pathological abnormalities were seen in any of the organs of sacrificed animals.

Discussion

A large number of studies carried out recently demonstrate the antimicrobial activity of aqueous suspensions of silver

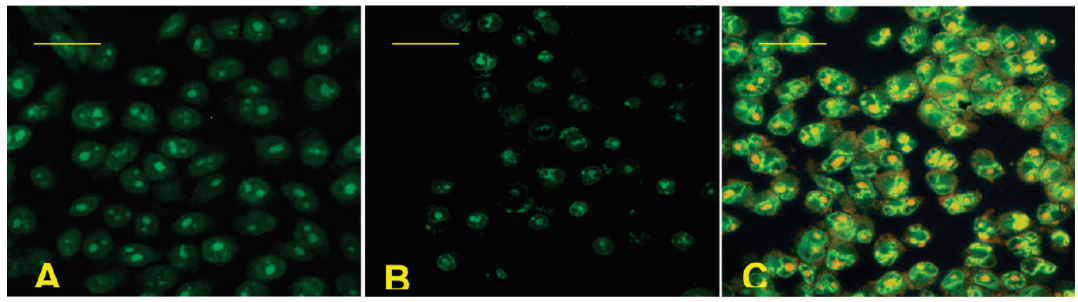

Figure 11. Confocal micrographs of acridine orange/ethidium bromide stained Hep G2 cells. (A) Unexposed (control) cells have a normal green nucleus indicating live cells. (B) Cells exposed to ~(1/2)IC_{50} SNP (125 μg/mL) for 24 h display bright green nucleus with condensed or fragmented chromatin suggesting apoptosis. (C) Cells exposed to ~2 × IC_{50} SNP (500 μg/mL) for 24 h have a structurally normal orange nucleus indicative of necrosis. Scale bar indicates 100 μm.

Table 5. Quantification of AO/EB Stained Hep G2 Cells (%)[a] after Exposure to SNP (~(1/2)IC_{50} SNP and 2 × IC_{50}) for 24 h

type of cells	control (unexposed) cells	exposed to ~(1/2)IC_{50} SNP (125 μg/mL)	exposed to ~2 × IC_{50} SNP (500 μg/mL)
live cells	96 ± 3	67 ± 5*	53 ± 6*
apoptotic cells	3 ± 2	28 ± 5*	11 ± 3*
necrotic cells	1 ± 1	5 ± 1*	36 ± 3*

[a] The data are expressed as mean ± standard deviation (SD) of three independent experiments. Asterisk (*) denotes a statistically significant difference compared to control ($p < 0.05$).

nanoparticles. Cho et al.[16] reported that poly-(*N*-vinyl-2-pyrrolidone) (PVP) stabilized silver nanoparticles showed MIC of 5 μg/mL against *S. aureus* and 10 μg/mL against *E. coli*. *S. aureus* and *E. coli* were completely inhibited at 50 and 100 μg/mL silver. Raffi et al.[17] reported that silver nanoparticles (mean size 16 nm) synthesized by inert gas condensation (IGC) method were effective bactericide against *Escherichia coli*, at concentration 60 μg/mL and higher. In another study, Shahverdi et al.[18] synthesized silver nanoparticles using culture supernatants of *Klebsiella pneumoniae* for reduction of aqueous Ag^+ ions. The antimicrobial activity of silver nanoparticles against *Staphylococcus aureus* and *Escherichia coli* was assessed by diffusion assay. It was also observed that activities of various antibiotics (penicillin G, amoxicillin, erythromycin, clindamycin, and vancomycin) were increased in the presence of silver nanoparticles. In the present study, MIC results obtained with SNP are comparable to those reported by Cho et al.[16] for PVP stabilized silver nanoparticles.

A study by Panacek et al.[19] described synthesis of silver nanoparticles of varying sizes (but narrow size distributions) using four different saccharides. The antimicrobial property of these nanoparticles against many Gram-positive and Gram-negative bacteria including multidrug-resistant strains was found to be size dependent. Nanoparticles with size >25 nm exhibited MIC of 6.75−54 μg/mL whereas 25 nm size particles showed MIC in the range of 1.69−13.5 μg/mL. The MIC results obtained with 25 nm particles are comparable to those obtained by us in the present study, where SNP suspension containing 7−20 nm particles were used. This is an important result, particularly when antibiotic resistance among bacterial species is increasing at an alarming rate and very few alternative options are available to address the issue. Park et al.[20] showed that hybrid silver (Ag) nanoparticles (size 3−7 nm) loaded on SiO_2 nanoparticles inhibited a range of standard fungi at concentration of 1 ppm. However, in our study, the obtained antifungal concentrations are 25-fold (~25 μg/mL). An interesting observation on variation in antimicrobial activity of silver nanoparticles due to strain specificity has been discussed by Ruparelia et al.[21] They showed that among the tested strains of *Escherichia coli* (four strains), *Bacillus subtilis* and *Staphylococcus aureus* (three strains), *Escherichia coli* strains showed maximum variation in the silver nanoparticle induced antimicrobial activity. Our results corroborate these findings as we find a lot of strain-dependent variation in antimicrobial response of SNP activity. In another study the MIC and MBC of Acticoat with *S. aureus*, *S. epidermidis*, *E. coli*, *K. aerogenes* and *P. aeruginosa* was reported to be 5−12.5 μg/mL,[22,23] which compares well with the results obtained with SNP. It was reported that

(16) Cho, K. H.; Park, J. E.; Osaka, T.; Park, S. G. The study of antimicrobial activity and preservative effects of nanosilver ingredient. *Electrochim. Acta* **2005**, *51*, 956–60.

(17) Raffi, M.; Hussain, F.; Bhatti, T. M.; Akhter, J. I.; Hameed, A.; Hasan, M. M. Antibacterial Characterization of Silver Nanoparticles against *E. coli* ATCC-15224. *J. Mater. Sci. Technol.* **2008**, *24*, 192–196.

(18) Shahverdi, A. R.; Fakhimi, A.; Shahverdi, H. R.; Minaian, S. Synthesis and effect of silver nanoparticles on the antibacterial activity of different antibiotics against Staphylococcus aureus and Escherichia coli. *Nanomed.: Nanotechnol., Biol., Med.* **2007**, *3*, 168–171.

(19) Panacek, A.; Kvitek, L.; Prucek, R.; Kolar, M.; Vecerova, R.; Pizurova, N.; Sharma, V. K.; Nevecna, T.; Zboril, R. Silver colloid nanoparticles: synthesis, characterization, and their antibacterial activity. *J. Phys. Chem. B* **2006**, *110*, 16248–16253.

(20) Park, H.-J.; Kim, H. J.; Kim, S. H.; Oh, S.-D.; Choi, S.-H. Radiolytic synthesis of hybrid silver nanoparticles and their biobehavior. *Key Eng. Mater.* **2007**, *342−343*, 897–900.

(21) Ruparelia, J. P.; Chatterjee, A. K.; Duttagupta, S. P.; Mukherji, S. Strain specificity in antimicrobial activity of silver and copper nanoparticles. *Acta Biomaterialia* **2008**, *4*, 707–716.

(22) Burrel, R. E.; McIntosh, C. L.; Morris, I. R. Process of activating antimicrobials materials. 1995, US Patent 5,455,886.

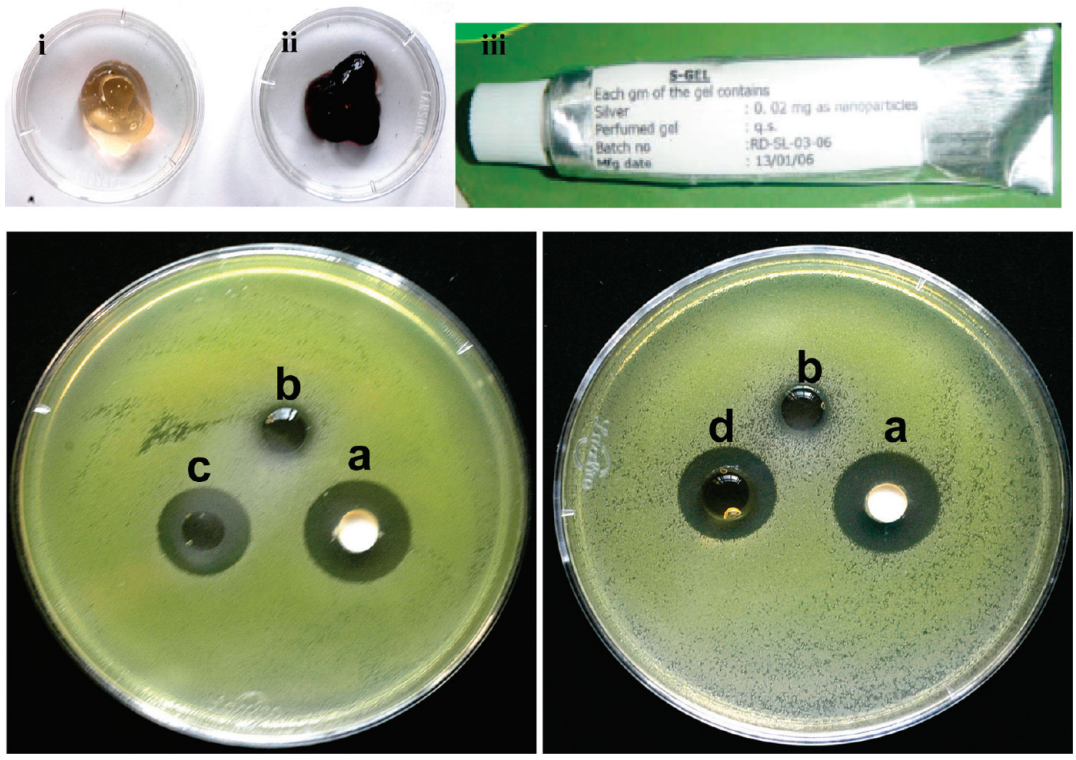

Figure 12. SNP containing formulation (S-gel) and its antimicrobial activity. S-gel with SNP concentration of 0.02 mg/g (i) and 0.1 mg/g (ii) and typical packaged product (iii). Zones of inhibition shown by 1% silver sulfadiazine (a), control gel without SNP (b) and S-gel with SNP concentration of 0.02 mg/g (c) and 0.1 mg/g (d).

Table 6. Sensitivity Zones of Topical Antibacterial Agents against Standard Bacterial Cultures and MDR Clinical Isolates

	zone diameter (zone size in mm*)		
	S-gel		
organism tested	0.02 mg/g	0.1 mg/g	1% silver sulfadiazine
E. coli ATCC 117	3	5	6
P. aeruginosa ATCC 9027	10	13	13
S. aureus ATCC 6538	5	6	9
B. subtilis ATCC 6633	6	8	12
P. vulgaris NCIB 4157	5	8	12
S. abony NCTC 6017	3	6	8
S. typhimurium ATCC 23564	5	9	13
K. aerogenes ATCC 1950	9	9	13
S. epidermidis ATCC 12228	4	6	8
Pseudomonas sp. # 1 MDR	10	13	13
Staphylococococcus sp. # 1 MDR	4	6	8

*Corrected zone of inhibition = (diameter of inhibited area − diameter of well).

the concentration of silver released from Acticoat is normally in the range of 60−80 μg/mL,[24] which helps achieve killing of the organisms within 30 min. In comparison, SNP require 6−8 h for killing most bacterial strains (please see data on MBC) but the concentration of silver released is very low (below the detection limit of a sensitive atomic absorption spectrophotometer—unpublished data).

The rationale of the FICI study considered two possibilities, viz., (a) adverse effect on the antimicrobial action of SNP in the presence of commonly used antibiotics and (b) beneficial effect of certain antibiotics in combination with SNP to provide enhanced and broad spectrum antimicrobial to handle infections of mixed etiology. Our results showed an antagonistic effect of SNP−chloramphenicol combination. On the other hand, additive and synergistic effects were seen for SNP combinations with streptomycin, kanamycin, polymyxin B sulfate, ampiclox and ceftazidime. These results suggest that, in the future, such combinations could be developed for getting more effective formulations. Combined antimicrobial activity of silver−water dispersion (colloidal silver) and antibiotics against seven bacterial strains was studied by de Souza et al.[25] and reported synergistic combination with amikacin and cefoperazone.

The post agent effect (PAE) is an important pharmacodynamic parameter investigated during the development of an antimicrobial agent. It contributes to the choice of antimicrobial dosing regimens and is defined as length of time that bacterial growth is suppressed following brief exposure to the antimicrobial agent. Generally, the PAE

(23) Yin, H. Q.; Langford, R.; Burrell, R. E. Comparative evaluation of the antimicrobial activity of Acticoat™ antimicrobial barrier dressing. *J. Burn Care Rehab.* **1999**, *20*, 195–200.

(24) Wright, J. B.; Hansen, D. L.; Burrell, R. E. The comparative efficacy of two antimicrobial barrier dressings. *Wounds* **1998**, *l0*, 179–188.

(25) de Souza, A.; Mehta, D.; Leavitt, R. W. Bactericidal activity of combinations of Silver-Water Dispersion with 19 antibiotics against seven microbial strains. *Curr. Sci.* **2006**, *91*, 926–929.

observed with specific antimicrobial agent−organism combinations ranges from 0.5 to 6 h. Antibiotics which inhibit protein and nucleic acid synthesis tend to produce longer PAEs, as compared to those which act on cell wall synthesis.[26] The prolonged PAE ranging from 4 to 11 h for Gram-negative organisms observed with SNP may be attributed to the inactivation of proteins. Direct evidence of protein inactivation by silver nanoparticles has been recently provided by Lok et al.[27] Our results suggest that longer dosing interval may be possible because the majority of tested strains have PAE >3 h. We believe that PAE of silver nanoparticles is being demonstrated for the first time.

The anti-inflammatory effects of silver ion on a wound have been recognized for centuries. Most of the reports are purely descriptive in nature, identifying the decrease in erythema and increased healing. A number of the biochemical effects of silver on the wound have been documented over a decade ago. There is an increased expression of matrix metalloproteinases (MMPs) in a burn wound and in chronic wounds.[28] Excess proteinase activity is now considered to be a major cause of impaired healing by destroying new tissue and growth factors. Matrix metalloproteinases such as collagenases (MMP-1) (MMP-8), gelatinases (MMP-2 and -9), stromelysin (MMP-3) and elastase (MMP-13) are especially found in burn wounds. In the present study a quantitative assay was undertaken using MMP-2 (gelatinase A) and MMP-9 (gelatinase B). As collagenase MMP-1, MMP-8, and MMP-13 have related activities, they are anticipated to behave similarly and produce results similar to those obtained for the gelatinase tested. The dose-dependent inhibition of both MMP-2 and MMP-9 with SNP demonstrates anti-inflammatory response which may enhance wound healing in vivo.

In vitro studies on exposure of cell lines (C18-4 germ cell line, BRL 3A liver cell line and PC-12 neuroendocrine cell line) to silver nanoparticles have shown decreased mitochondrial function and induction of apoptosis or apoptosis-like change of cell morphology.[29−31] In the event of entry of nanoparticles into the systemic circulation, they are likely to get distributed throughout the body; specifically in liver, which is a major accumulation site for toxic chemicals. Therefore, liver cells (rodent or human origin) represent a useful tool for studying toxicity, drug metabolism, and enzyme induction.[32,33] Liver cell line, viz., Hep G2, has been used for assessment of in vitro genotoxicity[34] and cytotoxicity[35] of many toxic agents as well as nanoparticles.[36] Considering these facts, Hep G2 cells were selected for evaluation of in vitro toxicity of SNP.

The toxicity of SNP was evaluated by studying specific mitochondrial marker (XTT assay) under control and exposed conditions. Results obtained by us clearly showed decreased mitochondrial function in cells exposed to SNP (12.5−400 μg/mL) in a dose-dependent manner as evidenced in the XTT assay. The IC_{50} value of SNP was found to be 251 μg/mL. This higher IC_{50} value is probably an inherent characteristic of Hep G2, because our earlier studies with established cell lines derived from human skin carcinoma and human fibrosarcoma[37] show lower IC_{50} value. Apart from this, studies on localization of silver nanoparticles were carried out by transmission electron microscopy after exposing the cells to SNP, since at this stage, it was not known whether these SNP are interacting with cells physically by getting lodged on the cell surface or are translocated inside the cells. Ultrathin sections of Hep G2 cells exposed to $\sim(1/2)IC_{50}$ SNP for 24 h, visualized under transmission electron microscope, showed the presence of dark, electron dense, spherical aggregates inside the mitochondria. These structures could probably be silver nanoparticles. Our results are in agreement with earlier reports where nanosized particles of various chemistries were shown to mobilize into mitochondria preferentially.[38,39] Mitochondria represent the most active cellular redox organelle, and localization of these particles into such redox active centers is expected to cause

(26) MacKenzie, F. M.; Gould, I. M. The post-antibiotic effect. *J. Antimicrob. Chemother.* **1993**, *32*, 519–537.
(27) Lok, C. N.; Ho, C. M.; Chen, R.; Qing-Yu, H.; Yiu, Y. W.; Sun, H.; Tam, P. K. H.; Chiu, J. F.; Che, C. M. Proteomic analysis of the mode of antibacterial action of silver nanoparticles. *J. Proteome Res.* **2006**, *5*, 915–924.
(28) Demling, R. H.; DeSanti, L. Effects of silver on wound management. *Wounds* **2001**, *13*, 4–9.
(29) Braydich-Stolle, L.; Hussain, S.; Schlager, J. J.; Hofmann, M. C. In vitro cytotoxicity of nanoparticles in mammalian germline stem cells. *Toxicol. Sci.* **2005**, *88*, 412–419.
(30) Hussain, S. M.; Hess, K. L.; Gearhart, J. M.; Geiss, K. T.; Schlager, J. J. In vitro toxicity of nanoparticles in BRL 3A rat liver cells. *Toxicol. in Vitro* **2005**, *19*, 975–983.
(31) Hussain, S. M.; Javorina, A. K.; Schrand, A. M.; Duhart, H. M.; Ali, S. F.; Schlager, J. J. The interaction of manganese nanoparticles with PC-12 cells induces dopamine depletion. *Toxicol. Sci.* **2006**, *92*, 456–463.
(32) Davila, J. C.; Acosta, D. Preparation of primary monolayer of postnatal rat liver cells for hepatotoxicity assessment of xenobiotics. In *In Vitro Biological Systems*, Tyson, C. A., Frazier, J. M., Eds.; Academic: San Diego, 1993; pp 244−261.
(33) Zurlo, J.; Arterburn, L. M. Characterization of a primary hepatocyte culture system for toxicological studies. *In Vitro Cell Dev. Biol.* **1996**, *32*, 211–220.
(34) Bhatt, T. S.; Coombs, M.; DiGiovanni, J.; Diamond, L. Mutagenesis in Chinese hamster cells by cyclopenta(α)phenanthrenes activated by a human hepatoma cell line. *Cancer Res.* **1983**, *43*, 984–986.
(35) Babich, H.; Sardana, M. K.; Borenfreund, E. Acute cytotoxicities of polynuclear aromatic hydrocarbons determined in vitro with the human liver tumor cell line Hep G2. *Cell Biol. Toxicol.* **1988**, *4*, 295–309.
(36) Ponti, J.; Colognato, R.; Franchini, F.; Gioria, S.; Simonelli, F.; Abbas, K.; Rossi, F. Uptake and cytotoxicity of gold nanoparticles in MDCK and HepG2 cell lines. http://www.aist-riss.jp/projects/nedo-nanorisk/nanorisk_symposium2008/pdf/03_122_en_ROSSI.pdf. 2008. Accessed Jan 9, 2009.
(37) Arora, S.; Jain, J.; Rajwade, J. M.; Paknikar, K. M. Cellular responses induced by silver nanoparticles: *In vitro* studies. *Toxicol. Lett.* **2008**, *179*, 93–100.
(38) Foley, S.; Crowley, C.; Smaihi, M.; Bonfils, C.; Erlanger, B. F.; Seta, P. Cellular localization of a water-soluble fullerene derivative. *Biochem. Biophys. Res. Commun.* **2002**, *294*, 116–119.

alterations in various antioxidant enzyme systems. Further, ROS production has been found in nanoparticles as diverse as C60 fullerenes,[40] single-walled carbon nanotubes,[41] quantum dots,[42] and ultrafine particles.[43] Studies on rat liver derived cell line (BRL 3A) showed that there was a significant increase in ROS and decrease in GSH levels at 25 and 50 μg/mL of Ag (15, 100 nm).[30] A significant elevation of lipid peroxidation and marginal GSH depletion was demonstrated in a fish model upon exposure to fullerenes.[40] Therefore levels of antioxidant enzymes, viz., catalase, superoxide dismutase, glutathione reduced content, glutathione peroxidase and lipid peroxidation, were monitored after exposing the cells to $\sim$(1/2)IC_{50} (125 μg/mL) SNP in the present study. The results obtained, i.e., enhancement of GSH ($\sim$1.1-fold), catalase ($\sim$1.1-fold) and SOD ($\sim$1.4-fold), indicated that Hep G2 cells were protected from oxidative stress. Thus, oxidative stress due to SNP does not persist long enough to cause oxidative damage to Hep G2 cells.

It is now well established that the generation or external addition of ROS can cause cell death by two distinct cell death pathways, viz., apoptosis or necrosis. Necrosis is detrimental for wound healing and often results in healing with scar formation.[44] ROS are known to activate caspases, which are considered as the executioners of apoptosis.[45,46] Involvement of caspases in silver nanoparticles mediated apoptosis in the baby hamster kidney (BHK21) and human colon adenocarcinoma (HT29) cell lines has also been shown.[47] The correlation between oxidative stress and apoptosis, as explained above, prompted us to investigate the type of cell death in SNP toxicity.

The type of cell death after SNP exposure was evaluated by caspase-3 activity assays, fluorescence microscopy and CLSM studies. Caspase-3 activity assay data clearly show that, at concentrations up to 250 μg/mL, cell death occurs mainly due to apoptosis. Cytotoxicity (necrosis) at higher doses of SNP (>250 μg/mL) could be clearly demonstrated by total lack of caspase-3 activity. Fluorescence light microscopy with differential uptake of fluorescent DNA binding dyes (AO/EB staining) is a method of choice (for its simplicity, rapidity, and accuracy) that distinguishes between apoptotic and necrotic cell populations. Acridine orange (AO) permeates all cells and makes the nuclei appears green. Ethidium bromide (EB) is only taken up by cells when cytoplasmic membrane integrity is lost, and stains the nucleus red. EB also dominates over AO. Thus live cells have a normal green nucleus; early apoptotic cells have bright green nucleus with condensed or fragmented chromatin; late apoptotic cells display condensed and fragmented orange chromatin; cells that have died from direct necrosis have a structurally normal orange nucleus.[48] To support these findings, typical apoptotic or necrotic features in cells were also observed under CLSM. Apoptotic cell population is higher at $\sim$(1/2)IC_{50} SNP and necrotic cell population is several fold ($\sim$7-fold) higher at $\sim 2 \times IC_{50}$ SNP. Apoptotic cell death would not lead to undesirable side reactions that are predominant during necrosis. Similar studies were done on the baby hamster kidney (BHK21) and human colon adenocarcinoma (HT29) cell lines where necrotic cell death was observed at silver nanoparticle concentrations >44.0 μg/mL.[47] Results obtained in the present study indicate safety of SNP even at $\sim$(1/2)IC_{50} SNP (251 μg/mL) concentration in liver derived cells.

The data on PAE indicated that dose regimen of the SNP formulation should ensure sustained release of the drug, and hence a formulation (S-gel) containing SNP for topical application was developed. At higher concentration of silver (0.1 mg/g) in S-gel, a significantly wider zone of inhibition was observed than that with the S-gel containing less silver, indicating a dose-dependent activity. When a standard commercial preparation, 1% silver sulfadiazine (SSD), was tested against *P. aeruginosa*, the inhibition zone was 23 mm, which was similar to S-gel (0.1 mg/g), indicating that S-gel formulation showed antibacterial activity, comparable to silver sulfadiazine albeit at 30-fold less silver concentration.

The wound healing properties of silver nanoparticles in an animal model and rapid healing and better cosmetic appearance in a dose-dependent manner were observed by

(39) Li, N.; Sioutas, C.; Cho, A.; Schmitz, D.; Misra, C.; Sempf, J. Ultrafine particulate pollutants induce oxidative stress and mitochondrial damage. *Environ. Health Perspect.* **2003**, *111*, 455–460.

(40) Oberdorster, G.; Sharp, Z.; Atudorei, V.; Elder, A.; Gelein, R.; Kreyling, W.; Cox, C. Translocation of inhaled ultrafine particles to the brain. *Inhalation Toxicol.* **2004**, *16*, 437–445.

(41) Shvedova, A. A.; Kisin, E.; Keshava, N.; Murray, A. R.; Gorelik, O.; Arepalli, S. Cytotoxic and genotoxic effects of single wall carbon nanotube exposure on human Keratinocytes and bronchial epithelial cells [Abstract]. In *Abstracts of Papers*, 227th National Meeting of the American Chemical Society, Anaheim, CA, 27 March−1 April 2004; American Chemical Society: Washington, DC, 2004; IEC 20.

(42) Derfus, A. M.; Chan, W. C. W.; Bhatia, S. N. Probing the cytotoxicity of semiconductor quantum dots. *Nano Lett.* **2004**, *4*, 11–18.

(43) Brown, D. M.; Wilson, M. R.; MacNee, W.; Stone, V.; Donaldson, K. Size-dependent proinflammatory effects of ultrafine polystyrene particles: a role for surface area and oxidative stress in the enhanced activity of ultrafines. *Toxicol. Appl. Pharmacol.* **2001**, *175*, 191–199.

(44) Tian, J.; Wong, K. K. Y.; Ho, C. M.; Lok, C. N.; Yu, W. Y.; Che, C. M.; Chiu, J. F.; Paul, K. H. T. Topical delivery of silver nanoparticles promotes wound healing. *ChemMedChem* **2007**, *2*, 129–136.

(45) Cohen, G. M. Caspases: the executioners of apoptosis. *Biochem. J.* **1997**, *326*, 1–16.

(46) Fadeel, B.; Ahlin, A.; Henter, J. I.; Orrenius, S.; Hampton, M. B. Involvement of caspases in neutrophil apoptosis: regulation by reactive oxygen species. *Blood* **1998**, *92*, 4808–4818.

(47) Gopinath, P.; Gogoi, S. K.; Chattopadhyay, A.; Ghosh, S. S. Implications of silver nanoparticle induced cell apoptosis for in vitro gene therapy. *Nanotechnology* **2008**, *19*, 1–10.

(48) Renvoize, C.; Biola, A.; Pallardy, M.; Breard, J. Apoptosis: Identification of dying cells. *Cell Biol. Toxicol.* **1998**, *14*, 111–120.

Wong et al.[49] Furthermore, through quantitative PCR, immunohistochemistry, and proteomic studies, the authors showed that silver nanoparticles exerted positive effects through their antimicrobial properties, reduction in wound inflammation, and modulation of fibrogenetic cytokines. In the present study, apart from antimicrobial activity, in vitro inhibition of MMPs was also proved. The in vitro studies in an established cell line, Hep G2, also indicate that concentrations that are typically antimicrobial are non-cytotoxic and would promote scarless wound healing. Further, the acute dermal LD_{50} value of S-gel in Sprague−Dawley rats, both male and female, was found to be greater than 2000 mg/kg body weight. Also, no mortality or signs of local or systemic toxicity and pathological abnormalities were seen, indicating safety at the highest concentration tested.

(49) Wong, K. K. Y.; Tian, J.; Ho, C.; Lok, C.; Che, C.; Che, J.-F.; Tam, P. K. H. Topical delivery of silver nanoparticles reduces systemic inflammation of burn and promotes wound healing. Concurrent Symposium XX: Nanotechnology in Biomedical and Clinical Application.

In conclusion, our study offers an unequivocal proof that SNP work as a potent antimicrobial agent at low concentrations. In vitro and in vivo experiments established the safety of SNP as well as its formulation (S-gel). The latter could be an effective and safer alternative to conventional topical antimicrobial agents, especially for treating burn wounds.

Acknowledgment. The authors acknowledge financial support from Nano Cutting Edge Technology Pvt. Ltd., Mumbai. J.J. thanks Indian Council of Medical Research (ICMR), New Delhi, for a research fellowship. S.A. thanks Council of Scientific and Industrial Research (CSIR), New Delhi, for a research fellowship. The authors are thankful to Interactive Research School for Health Affairs (IRSHA), Pune, for providing animal tissue culture facility and National Center for Cell Sciences (NCCS), Pune, for confocal laser scanning microscopy (CLSM).

MP900056G